

# Construction of a pH-Driven Supramolecular Nanovalve

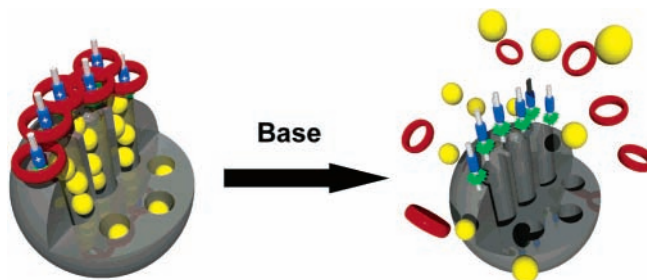
Thoi D. Nguyen, Ken C.-F. Leung, Monty Liong, Cari D. Pentecost, J. Fraser Stoddart,\* and Jeffrey I. Zink\*

California NanoSystems Institute and Department of Chemistry and Biochemistry, University of California, Los Angeles, 405 Hilgard Avenue, Los Angeles, California 90095

stoddart@chem.ucla.edu; zink@chem.ucla.edu

Received May 22, 2006

## ABSTRACT



The versatility of supramolecular chemistry has been exploited in constructing nanovalves based on mesoporous silica MCM-41 and the mutual recognition between secondary dialkylammonium ions and dibenzo[24]crown-8 (DB24C8). Naphthalene-containing dialkylammonium threads were tethered to the MCM-41, followed by loading with coumarin 460 and capping with DB24C8. Controlled release of coumarin 460 from the pores of MCM-41 was demonstrated using different bases. The rate of release of coumarin 460 from the nanovalves depends on the size of the base.

One of the toughest challenges today for researchers intent upon taking chemistry up to the frontiers of nanoscience is to introduce a rather fine level of control upon nanoscale devices adorned with molecular machinery<sup>1</sup> that has been designed and self-assembled to fulfill a particular device function. Prominent among such hybrid systems are supramolecular<sup>2</sup> and molecular<sup>3</sup> valves with movable elements that can be grafted onto mesoporous silica reservoirs in such

a manner that the two parts will work together in harmony to achieve some desirable outcome at the macroscopic level. Molecules with movable elements, which have been incorporated into working devices, include (1) azobenzene derivatives<sup>4a</sup> which can be induced to undergo *cis*–*trans* isomerization, (2) coumarin derivatives<sup>4b</sup> which can be made to display reversible intermolecular dimerization, (3) derivatized CdS nanoparticles<sup>4c</sup> that are chemically labile thanks to the reversibility of the thiol/disulfide redox process, (4) heat-responsive<sup>4d</sup> polymers which are extended at high and collapsed at low temperatures, (5) electrically erodible

(1) (a) Balzani, V.; Credi, A.; Raymo, F. M.; Stoddart, J. F. *Angew. Chem., Int. Ed.* **2000**, *39*, 3348–3391. (b) Balzani, V.; Credi, A.; Venturi, M. *Molecular Devices and Machines: A Journey into the Nano World*; Wiley-VCH: Weinheim, Germany, 2003. (c) Badjić, J. D.; Balzani, V.; Credi, A.; Silvi, S.; Stoddart, J. F. *Science* **2004**, *303*, 1845–1849. (d) Collin, J.-P.; Heitz, V.; Sauvage, J.-P. *Top. Curr. Chem.* **2005**, *262*, 29–62. (e) Kay, E. R.; Leigh, D. A. *Top. Curr. Chem.* **2005**, *262*, 133–177. (f) Braunschweig, A. B.; Northrop, B. H.; Stoddart, J. F. *J. Mater. Chem.* **2006**, *16*, 32–44.

(2) Hernandez, R.; Tseng, H.-R.; Wong, J. W.; Stoddart, J. F.; Zink, J. I. *J. Am. Chem. Soc.* **2004**, *126*, 3370–3371.

(3) Nguyen, T. D.; Tseng, H.-R.; Celestre, P. C.; Flood, A. H.; Liu, Y.; Stoddart, J. F.; Zink, J. I. *Proc. Natl. Acad. Sci. U.S.A.* **2005**, *102*, 10029–10034.

(4) (a) Liu, N.; Dunphy, D. R.; Atanassov, P.; Bunge, S. D.; Chen, Z.; López, G. P.; Boyle, T. J.; Brinker, C. J. *Nano Lett.* **2004**, *4*, 551–554. (b) Mal, N. K.; Fujiwara, M.; Tanaka, Y. *Nature* **2003**, *421*, 350–353. (c) Lai, C.-Y.; Trewyn, B. G.; Jęftinija, D. M.; Jęftinija, K.; Xu, S.; Jęftinija, S.; Lin, V. S.-Y. *J. Am. Chem. Soc.* **2003**, *125*, 4451–4459. (d) Fu, Q.; Rama Rao, G. V.; Ista, L. K.; Wu, Y.; Andrzejewski, B. P.; Sklar, L. A.; Ward, T. L.; López, G. P. *Adv. Mater.* **2003**, *15*, 1262–1266. (e) Kwon, I. C.; Bae, Y. H.; Kim, S. W. *Nature* **1991**, *354*, 291–293. (f) Rudzinski, W. E.; Chipuk, T.; Dave, A. M.; Kumbhar, S. G.; Aminabhavi, T. M. *J. Appl. Polym. Sci.* **2003**, *87*, 394–403.

polymer gel,<sup>4e</sup> and (6) pH-sensitive copolymeric hydrogels.<sup>4f</sup> Other wholly inorganic systems involve<sup>5</sup> the electrochemical corrosion of a gold membrane in microelectromechanical systems to open the valve. In all cases, the movable elements operate in response to a single response.

A unique class of molecules with switchable, and hence movable, elements are the mechanically interlocked ones, such as bistable catenanes and rotaxanes.<sup>6</sup> These compounds can be designed such that their movable elements can be controlled<sup>7</sup> by external stimuli, such as pH, electricity, or light. We have recently reported<sup>3</sup> that donor–acceptor bistable [2]rotaxanes can be tethered to porous silica thin films and MCM-41 to act together as molecular valves. The analogous situation exists in the supramolecular domain where [2]pseudorotaxanes act as gatekeepers at the orifices to the pores. The mode of action of these two valves relies on the redox switching of the ring in order to move it away from the entrances to the orifices, thus allowing release of the contents trapped inside the pores. Herein, we report the synthesis and operation of a supramolecular valve that relies on the pH-controllable crown ether/dialkylammonium ion-based recognition motif<sup>8</sup> as the driving force for pseudorotaxane formation.

Dibenzo[24]crown-8 (DB24C8) is a sufficiently large macrocyclic polyether to be able to encircle dialkylammonium ion centers ( $-\text{CH}_2\text{NH}_2^+\text{CH}_2-$ ), thus forming [2]pseudorotaxanes.<sup>8</sup> Since the noncovalent bonding responsible for the formation of these 1:1 complexes involves, inter alia,  $[\text{N}-\text{H}\cdots\text{O}]^+$  hydrogen bonds, they can be made to dissociate in solution on addition of base. In the context of the present work, that is, constructing pH-driven supramolecular valves on the surface of mesoporous silica, the naphthalene-containing<sup>9</sup>  $-\text{CH}_2\text{NH}_2^+\text{CH}_2-$  tether, shown in the box in Figure 1, was utilized as the thread. The unthreaded form of the [2]pseudorotaxane at the high pH values represents the open state of the switch, while threading of the  $-\text{CH}_2\text{NH}_2^+\text{CH}_2-$  with DB24C8 beads closed the valve. Dethreading can be achieved using a range of bases.

Nanostructured silica, for use as both the solid support for the molecular machinery comprising the movable elements, and the containers in which guest molecules are

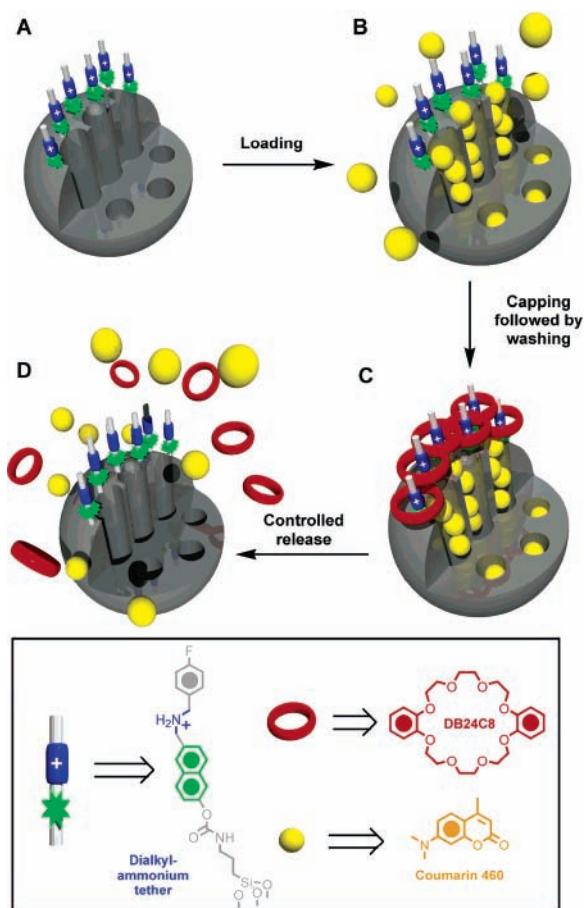


**Figure 1.** Graphical representations of operating (supra)molecular valves. The dialkylammonium-tethered porous silica particle MCM-41 (A) is loaded with coumarin 460 molecules (B). The pores of coumarin-loaded MCM-41 are capped with DB24C8 by noncovalent interactions, followed by washing away the excess of substrates (C). Coumarin 460 molecules are released by switching off the noncovalent interactions upon pH stimulation. (D) The porous silica particle MCM-41 can be reused for the next molecule-releasing cycle.

trapped and then released on demand, is prepared<sup>10,11</sup> by surfactant-directed self-assembly to yield ordered arrays of channels in sol–gel-derived silica. Using a modification of Stober’s synthesis of monodispersed silica for which aqueous ammonia was used as a morphology catalyst,<sup>11</sup> the nanostructured silica obtained consists of near-spherical silica particles with an average diameter of 600 nm, as verified (Figure 2) by scanning electron microscopy (SEM). Using cetyltrimethylammonium bromide as the template, the highly ordered pores form a two-dimensional hexagonal structure that has a lattice spacing of 3.6 nm as measured by X-ray diffraction (indexed as {100}). The surfactant was removed by calcination for 5 h at 550 °C. N<sub>2</sub> adsorption/desorption

(5) Santini, J. T., Jr.; Cima, M. J.; Langer, R. *Nature* **1999**, *397*, 335–338.

(6) (a) Flood, A. H.; Stoddart, J. F.; Steuerman, D. W.; Heath, J. R. *Science* **2004**, *306*, 2055–2056. (b) Mendez, P. M.; Flood, A. H.; Stoddart, J. F. *Appl. Phys. A* **2005**, *80*, 1197–1209. (c) Choi, J. W.; Flood, A. H.; Steuerman, D. W.; Nygaard, S.; Braunschweig, A. B.; Moonen, N. N. P.; Laursen, B. W.; Luo, Y.; Delonno, E.; Peters, A. J.; Jeppesen, J. O.; Xe, K.; Stoddart, J. F.; Heath, J. R. *Chem.–Eur. J.* **2006**, *12*, 261–279.

(7) (a) Bissell, R. A.; Córdova, E.; Kaifer, A. E.; Stoddart, J. F. *Nature* **1994**, *369*, 133–137. (b) Martínez-Díaz, M.-V.; Spencer, N.; Stoddart, J. F. *Angew. Chem., Int. Ed. Engl.* **1997**, *36*, 1904–1907. (c) Balzani, V.; Clemente-León, M.; Credi, A.; Semeraro, M.; Venturi, M.; Tseng, H.-R.; Wenger, S.; Saha, S.; Stoddart, J. F. *Aust. J. Chem.* **2006**, *59*, 193–206.

(8) (a) Glink, P. T.; Schiavo, C.; Stoddart, J. F.; Williams, D. J. *Chem. Commun.* **1996**, 1483–1490. (b) Hubin, T. J.; Kolchinski, A. G.; Vance, A. L.; Busch, D. H. *Adv. Supramol. Chem.* **1999**, *5*, 237–357. (c) Hubin, T. J.; Busch, D. H. *Coord. Chem. Rev.* **2000**, *200–202*, 5–52. (d) Cantrill, S. J.; Pease, A. R.; Stoddart, J. F. *J. Chem. Soc., Dalton Trans.* **2000**, 3715–3734. (e) Aricó, F.; Badjić, J. D.; Cantrill, S. J.; Flood, A. H.; Leung, K. C.-F.; Liu, Y.; Stoddart, J. F. *Top. Curr. Chem.* **2005**, *249*, 203–259.

(9) Williams, A. R.; Northrop, B. H.; Houk, K. N.; Stoddart, J. F.; White, A. J. P.; Williams, D. J. *Chem.–Eur. J.* **2004**, *10*, 5406–5421.

(10) (a) Kresge, C. T.; Leonowicz, M. E.; Roth, W. J.; Vartuli, J. C.; Beck, J. S. *Nature* **1992**, *359*, 710–712. (b) Lu, Y.; Ganguli, R.; Drewien, C. A.; Anderson, M. T.; Brinker, C. J.; Gong, W.; Guo, Y.; Soyez, H.; Dunn, B.; Huang, M. H.; Zink, J. I. *Nature* **1997**, *389*, 364–368.

(11) Grun, M.; Laner, I.; Unger, K. K. *Adv. Mater.* **1997**, *9*, 254–257.

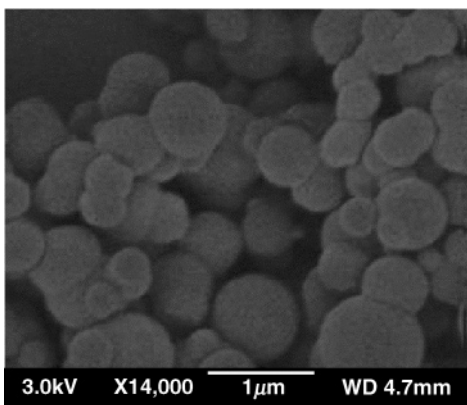


**Figure 2.** Scanning electron micrograph of the mesoporous silica particles. Note the 1  $\mu\text{m}$  scale bar.

isotherms at 77 K were used to investigate the porosity of the material further. The isotherm of the material can be classified as a type IV isotherm according to IUPAC nomenclature. The material exhibits high surface area (929.7  $\text{m}^2/\text{g}$ ). By employing the Barret–Joyner–Halenda (BJH) method of calculation, the inner diameter of the pore is estimated to be 2.0 nm.  $\text{N}_2$  adsorption/desorption isotherms also revealed that the pores are empty after calcination such that they are accessible and suitable for use as molecular containers (see Supporting Information).

The first step in the making of the supramolecular valve involves derivatizing the silanol functional groups on porous silica (MCM-41) with isocyanatopropyl–triethoxysilane (ICPES) to afford<sup>12a,b</sup> isocyanate-functionalized porous silica. In contrast to other one-pot syntheses,<sup>12c,d</sup> this grafting method for coupling a silane agent to the porous silica yields material with linkers predominantly situated either close to the pores' orifices or outside of the pores.<sup>12e,f</sup> The dialkylammonium ion's  $\beta$ -naphthol unit was then brought into contact with this surface, and a carbamate was formed, having, first of all, protected the secondary amine precursor of the ion with a *tert*-butoxycarbonyl group. Deprotection with trifluoroacetic acid produced (Figure 1A) the desired naphthalene-containing  $-\text{CH}_2\text{NH}_2^+\text{CH}_2-$  tethered MCM-41. The hybrid material was loaded subsequently (Figure 1B) with coumarin 460, and the pores were capped (Figure 1C) with DB24C8.

The operation of the nanovalve, that is, the release (Figure 1C,D) of the luminescent probe molecules (coumarin 460), was studied using luminescence spectroscopy. The loaded hybrid material was placed as a powder at the bottom of a spectrophotometric cell containing  $\text{CH}_2\text{Cl}_2$ , and only the solvent was exposed to excitation light. The solution was

stirred at a low stirring rate to create a homogeneous solution at any given time. The release of coumarin 460 molecules into the solvent was monitored by measuring the luminescence spectrum as a function of time. This task was achieved by using a charge-coupled device (CCD) detector. This CCD detector sequentially collects the luminescence spectra once per second, giving a three-dimensional plot of luminescence intensity, wavelength, and time, while confirming the identity of the molecules being released.

The effectiveness of the nanovalve depends on a number of factors. Its function depends critically on whether the movable elements associated with the [2]pseudorotaxanes can effectively prevent the probe molecules from leaking out. Equally important is the nanovalve's influence upon how efficient the opening and releasing of trapped guest molecules are from the pores. A range of bases with different basicities and structural dimensions, including hexamethylphosphorus triamide (HMPT), *N,N'*-diisopropylethylamine (DIPEA), and triethylamine (TEA), was employed to effect (Table 1) the

**Table 1.** Controlled Release Data for Base-Activated Valve with the Half-Life for the Release Corresponding to Each Base

	Base		
	HMPT	DIPEA	TEA
size <sup>a</sup> (nm)	6.2	5.9	5.8
half-life $t_{1/2}$ (s)	450	300	100

<sup>a</sup> Obtained from ChemDraw 3D.

controlled release of coumarin 460. The slight increase in the emission intensity (Figure 3) indicates a small amount of leakage from the closed nanovalve. The release of coumarin 460 from the pores upon activation by addition of HMPT (Figure 3A) was characterized by a lag time of 200 s. After this delay, the guest molecules were released at a much faster rate, as indicated by the much steeper slope. For HMPT-triggered release,<sup>13</sup>  $t_{1/2}$  is  $450 \pm 30$  s. The  $t_{1/2}$  for DIPEA-activated release (Figure 3B) is  $300 \pm 30$  s. With TEA as the base, no lag time is observed (Figure 3C) and the  $t_{1/2}$  decreases further to  $100 \pm 20$  s. All three samples were left to stand overnight, and the emission intensities were used to define the total (100%) amounts released.

Since all the experimental conditions to trigger the release of the guest molecules are the same, a direct comparison between the different release profiles, based on the nature of the triggering bases, can be made. Comparing the three bases, the controlled release—according to the deprotonation mechanism—is governed<sup>14</sup> by the basicity and the steric hindrance of the bases employed. DIPEA and TEA have similar basicities,<sup>15</sup> namely,  $\text{p}K_a = 9.0$  and 8.5, respectively, in  $\text{Me}_2\text{SO}$ . The rate of release using DIPEA is lower than

(12) (a) Haller, I. *J. Am. Chem. Soc.* **1978**, *100*, 8050–8055. (b) Chia, S.; Cao, J.; Stoddart, J. F.; Zink, J. I. *Angew. Chem., Int. Ed.* **2001**, *40*, 2447–2451. (c) Minoofar, P. N.; Hernandez, R.; Chia, S.; Dunn, B.; Zink, J. I.; Franville, A.-C. *J. Am. Chem. Soc.* **2002**, *124*, 14388–14396. (d) Hernandez, R.; Franville, A.-C.; Minoofar, P. N.; Dunn, B.; Zink, J. I. *J. Am. Chem. Soc.* **2001**, *123*, 1248–1249. (e) Lim, M. H.; Stein, A. *Chem. Mater.* **1999**, *11*, 3285–3295. (f) Lim, M. H.; Blanford, C. F.; Stein, A. *J. Am. Chem. Soc.* **1997**, *119*, 4090–4091.

(13) The half-life ( $t_{1/2}$ ) is defined as the time the system takes to release half of its load.

(14) Badjić, J. D.; Ronconi, C. M.; Stoddart, J. F.; Balzani, V.; Silvi, S.; Credi, A. *J. Am. Chem. Soc.* **2006**, *128*, 1489–1499.

(15) Lepore, S. D.; Khoram, A.; Bromfield, D. C.; Cohn, P.; Jairaj, V.; Silvestri, M. A. *J. Org. Chem.* **2005**, *70*, 7443–7446.



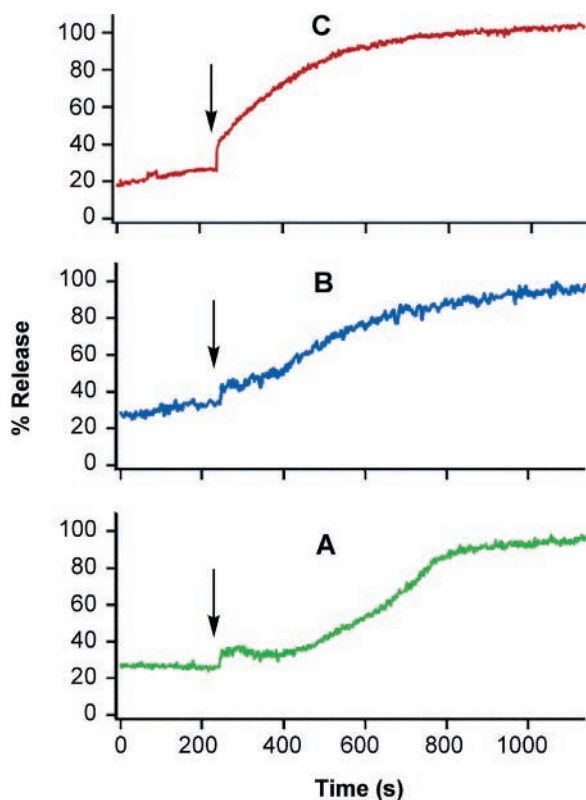


**Figure 3.** Controlled release of coumarin 460 from the dialkylammonium–DB24C8–MCM-41 nanovalve in  $\text{CH}_2\text{Cl}_2$  activated by (A) hexamethylphosphorus triamide, (B) *N,N'*-diisopropylethylamine, and (C) triethylamine, as monitored by luminescence spectroscopy over time. The arrow indicates the triggering time corresponding to 240 s.

that when using TEA. This result indicates that the more bulky DIPEA—despite being the stronger base—slows down the deprotonation of the complex tethered to the silica particles, thus affecting the rate of nanovalve operation (Table 1). When an even more bulky and weaker base (HMPT) is used,<sup>16</sup> the rate of release is even slower. HMPT- and DIPEA-activated releases exhibit lag times, whereas release

(16) Buntin, K. A.; Moreno, C.; Poč, A. J. *Dalton Trans.* **2005**, 1416–1421.

activated by TEA does not. The lag time observed for HMPT is longer than that for DIPEA, signifying a stronger impact on the part of steric hindrance. The variation of the bases having different steric factors and basicities, as a result, manifests itself in the three different release rates such that  $\text{TEA} > \text{DIPEA} > \text{HMPT}$ .

An alternative interpretation of the activation by TEA ( $\text{Et}_3\text{N}$ ) is that the nanovalve's operation is induced by a competitive binding mechanism involving DB24C8 and the tertiary trialkylammonium ion. However, when binding studies between DB24C8 and TEA and  $\text{Et}_3\text{NH}^+\cdot\text{CF}_3\text{CO}_2^-$  were performed, no interaction was observed, at least judging from  $^1\text{H}$  NMR spectroscopic data.<sup>17</sup> These results reveal that TEA acts as a base to deprotonate the  $-\text{CH}_2\text{NH}_2^+\text{CH}_2-$  ion center, hence releasing DB24C8 from the nanovalve. Extraction of the crown ether by a competitive binding mechanism is not happening.

The motion of the movable elements in the [2]pseudorotaxane tethered to a well-defined mesoporous nanostructure constitutes the open and closed configurations of this nanovalve system. The steric bulk of the bases plays a vital role in the functioning of the nanovalve and results in systems that can release guest molecules at different rates. Moreover, the diversity provided by different activating agents greatly improves the flexibility and applicability of this class of nanovalve. In principle, nanovalves having even larger pores could be mixed and matched with suitable [2]pseudorotaxanes to perform precise functions, such as targeted, acid–base-controlled drug delivery.

**Acknowledgment.** The research was conducted as part of an NSF-NIRT program and DMR 0346610. T.D.N. acknowledges support from the UCLA Dissertation Year Fellowship as well as assistance early on from Erik Johansson and Paul Sierocki.

**Supporting Information Available:** Preparative procedures of all precursor compounds and the nanovalve as well as the characterization data from NMR spectroscopy, XRD pattern, and  $\text{N}_2$  adsorption/desorption isotherm. This material is available free of charge via the Internet at <http://pubs.acs.org>.

OL0612509

(17) See Supporting Information.